Power System Dynamic State Estimation Based on Discretized Nonlinear Differential Algebraic Equation Models

Venkatanaga A. Aryasomyajula¹, Nikolaos Gatsis¹, and Ahmad F. Taha²

¹Department of Electrical and Computer Engineering, The University of Texas at San Antonio ²Department of Civil and Environmental Engineering, Vanderbilt University

Abstract—This paper investigates the use of nonlinear differential-algebraic equation (NDAE) models for dynamic state estimation (DSE) of power systems. NDAE models include dynamics of generators in multi-machine systems coupled with power flow equations. Although Numerical integration methods have contributed to solving NDAE models of power systems, NDAEs and the DSE problem have been treated separately in the majority of literature due to the complexity in solving NDAEs. In this paper, we leverage Gear's and trapezoidal methods to discretize NDAEs. This process combined with readings from phasor measurement units provides a model for DSE formulated as nonlinear least squares. The overall problem is solved using the Gauss-Newton method. The effectiveness and accuracy of the DSE is tested on standard test systems.

Index Terms—Differential Algebraic Equations, Dynamic State Estimation, Gauss-Newton method, Implicit Methods, Power Systems Dynamics.

I. INTRODUCTION

Power systems experience different types of uncertainty due to load changes and faults, thereby imposing various operational and stability-related challenges. Dynamic state estimation (DSE) is an effective tool for monitoring the dynamics of the system. Electromechanical transients and dynamics of multi-machine power systems are typically modeled by the power flow equations coupled with nonlinear differential and algebraic equations (NDAEs) pertaining to generators [1]–[4]. There are several numerical, hybrid, and decoupled methods to solve DAEs; see e.g., [5]–[8], but these methods have not been coupled with DSE. The present paper is specifically concerned with leveraging NDAEs for DSE based on readings from phasor measurement units (PMUs).

DAE models track the grid transients adequately for the purpose of performing DSE because, if DSE is performed only by using ordinary differential equation models, then PMU locations are restricted to generator buses [9]. The majority of the literature focuses mainly on the dynamical models of generators without placing particular emphasis on

This material is based upon work supported by the National Science Foundation under Grants CAREER-1847125 and ECCS-2115427. Emails: venkatanagaamrusha.aryasomyajula@utsa.edu, nikolaos.gatsis@utsa.edu, ahmad.taha@vanderbilt.edu.

978-1-6654-9921-7/22/\$31.00 ©2022 IEEE

the algebraic states of the network. For example, the works in [10], [11] only consider dynamics of generators obtained by Kron reduction. In [12], constant impedance loads are assumed to eliminate algebraic network equations of a DAE model and eventually avoid NDAEs. In [13], it is discussed that unless NDAEs are used, it is difficult to perform DSE whereby PMUs are installed on non-generator buses. To establish the relations between bus voltages at non-generator buses and generators' states, NDAEs are required. In [14], a distributed Gauss-Newton method to perform state estimation is developed, but the DAE model of the power system is not considered. Some works bypass the nonlinearities by linearizing the NDAEs around an equilibrium point [13], [15]. Despite their complexity, incorporating NDAE models into DSE is well motivated to enable the use of detailed generator models and power flow equations in addition to arbitrary PMU placement.

Numerous approaches have been proposed to solve the DSE problem. The works in [16], [17] are based on weighted least squares but do not consider readings from PMUs which measure nodal voltages and line currents. Kalman filter frameworks are introduced in [11], [18], [19], but the generator dynamical model is decoupled from the PMU model. Other approaches include observer-based frameworks [13], [20] and Newton-based methods [14], [21]. It is well known that the PMU measurement model is linear when nodal voltages are expressed in rectangular coordinates. If simplified dynamical models are considered—such as random walk for the voltages—then the DSE formulation is linear [22]. Instead, this paper adopts generator dynamics involving the swing equation and internal variables pertaining to the generator real and reactive power, which render the overall model nonlinear.

The present work develops a DSE problem capitalizing on a discretized power system NDAE model. The discretization is carried out using implicit numerical methods, namely, Gear's and trapezoidal methods. The overall problem is formulated as nonlinear least squares minimization and is solved using the Gauss-Newton method.

The remainder of this paper is organized as follows. The power system NDAE model, discretization of NDAEs, and the measurement model are presented in Section II. Section III formulates the objective function and develops the Gauss-Newton iterative method for the DSE problem. Section IV

provides numerical results regarding the performance of the proposed DSE approach using both discretization methods. The paper is concluded in Section V.

II. NONLINEAR DAE MODEL OF POWER SYSTEMS, DISCRETIZATION, AND MEASUREMENT MODEL

In this section, NDAE modeling of power systems and implicit discretization methods are detailed, followed by the measurement model.

A. NDAE model of Power Systems

The power network model consists of N buses with $\mathcal{G} = \{1, 2, ...G\}$ representing the set of buses connected to G synchronous generators. Set $\mathcal{L} = \{1, 2, ...L\}$ represents the buses containing loads only. Set \mathcal{N} consists of synchronous generators and load buses, i.e., $\mathcal{N} = \mathcal{G} \cup \mathcal{L}$. In this paper, we leverage a comprehensive 4th order one-axis generator dynamic model, generator's algebraic equations, and power flow equations. The dynamics of synchronous generator $i \in \mathcal{G}$ are written as [23]

$$\dot{\delta}_i = \omega_i - \omega_s \tag{1a}$$

$$M_i \dot{\omega}_i = T_{mi} - D_i (\omega_i - \omega_s) - P_{gi}$$
 (1b)

$$T'_{doi}\dot{e}_{i} = -\frac{x_{di}}{x'_{di}}e_{i} + \frac{x_{di} - x'_{di}}{x'_{di}}(v_{Ri}\cos(\delta_{i}) + v_{Ii}\sin(\delta_{i})) + E_{fdi}$$
(1c)

$$T_{Chi}\dot{T}_{mi} = T_{ri} - T_{mi} - \frac{1}{R_i}(\omega_i - \omega_s)$$
 (1d)

where $\delta_i = \delta_i(t)$ is the rotor angle (rad), $\omega_i = \omega_i(t)$ is the rotor speed (rad/sec), $e_i = e_i(t)$ is the generator transient voltage (pu), $T_{mi} = T_{mi}(t)$ is the mechanical input power (pu), $v_{Ri} = v_{Ri}(t)$ and $v_{Ii} = v_{Ii}(t)$ are real and imaginary generator terminal voltages (pu), $E_{fdi} = E_{fdi}(t)$ is the generator internal field voltage (pu), and $T_{ri} = T_{ri}(t)$ is the generator reference signal (pu). The constants in (1) are defined as follows: M_i is the rotor inertia (pu \times sec²), D_i is the generator damping coefficient (pu \times sec), x'_{di} is the direct-axis transient reactance (pu), x_{di} is the direct-axis synchronous reactance (pu), T'_{doi} is the direct-axis open circuit time constant (sec), T_{Chi} is the chest valve time constant (sec), R_i is the speed governor regulation constant in $(\frac{\text{rad} \times \text{Hz}}{\text{pu}})$, and ω_s is the rotor synchronous speed (rad/sec).

The algebraic equations represent the relation among the generator dynamic states, real and reactive power (P_{gi}, Q_{gi}) (pu), and real and imaginary terminal voltages (v_{Ri}, v_{Ii}) . The two algebraic equations for $i \in \mathcal{G}$ are stated as [23]

$$0 = \frac{e_i}{x'_{di}} (v_{Ri} \sin(\delta_i) - v_{Ii} \cos(\delta_i))$$

$$- \frac{x_{qi} + x'_{di}}{2x'_{di}x_{qi}} ((v_{Ri}^2 - v_{Ii}^2) \sin(2\delta_i) - 2v_{Ri}v_{Ii} \cos(2\delta_i)) - P_{gi}$$
(2a)
$$0 = \frac{e_i}{x'_{di}} (v_{Ri} \cos(\delta_i) + v_{Ii} \sin(\delta_i)) - \frac{x'_{di} - x_{qi}}{2x'_{di}x_{qi}} (v_{Ri}^2 + v_{Ii}^2)$$

$$+ \frac{x'_{di} - x_{qi}}{2x'_{di}x_{qi}} (v_{Ri}^2 \cos(2\delta_i) - v_{Ii}^2 \cos(2\delta_i)$$

$$+2v_{Ri}v_{Ii}\sin(2\delta_i)) - Q_{ai} \tag{2b}$$

where x_{qi} is the quadrature-axis synchronous reactance (pu). The network power flow equations for bus $i \in \mathcal{N}$ are [23]

$$P_{li} - P_{gi} + \sum_{j=1}^{N} G_{ij}(v_{Ri}v_{Rj} + v_{Ii}v_{Ij})$$

$$+ B_{ij}(v_{Ii}v_{Rj} - v_{Ri}v_{Ij}) = 0$$

$$Q_{li} - Q_{gi} + \sum_{j=1}^{N} G_{ij}(v_{Ii}v_{Rj} - v_{Ri}v_{Ij})$$

$$- B_{ij}(v_{Ri}v_{Rj} + v_{Ii}v_{Ij}) = 0$$
(3b)

where G_{ij} and B_{ij} are respectively the conductance and susceptance of the line between buses i and j, P_{li} and Q_{li} are the active and reactive power consumed by the loads (pu). If a bus does not have loads, P_{li} and Q_{li} are set to zero.

Each synchronous generator has four dynamic states, which are all collected in $\boldsymbol{x} = [\boldsymbol{\delta}_i^T \ \boldsymbol{\omega}_i^T \ \boldsymbol{e}_i^T \ \boldsymbol{T}_{mi}^T]^T$, whereas generators' internal field voltage and reference signal are considered control inputs, i.e., $\boldsymbol{u} = [\boldsymbol{E}_{fdi}^T \ \boldsymbol{T}_{ri}^T]^T$. The algebraic state representing the generators' powers is defined as $\tilde{\boldsymbol{a}} = [\boldsymbol{P}_g^T \ \boldsymbol{Q}_g^T]^T$ where $\boldsymbol{P}_g = \{\boldsymbol{P}_{gi}\}_{i\in\mathcal{G}}, \boldsymbol{Q}_g = \{\boldsymbol{Q}_{gi}\}_{i\in\mathcal{G}}$ and the algebraic state representing the network's bus voltages in rectangular form is defined as $\tilde{\boldsymbol{v}} = [\boldsymbol{v}_R^T \ \boldsymbol{v}_I^T]^T$ where $\boldsymbol{v}_R = \{\boldsymbol{v}_{Ri}\}_{i\in N}, \boldsymbol{v}_I = \{\boldsymbol{v}_{Ii}\}_{i\in N}$. The algebraic states together are collected in $\boldsymbol{a} = [\tilde{\boldsymbol{a}}^T \ \tilde{\boldsymbol{v}}^T]^T$. Based on the previously defined vectors, the complete NDAE model (1)–(3) is

NDAE:
$$\dot{x} = f(x, a, u)$$
 (4a)

$$\mathbf{0} = \mathbf{g}(\mathbf{x}, \mathbf{a}) \tag{4b}$$

where the vector-valued functions f and g represent differential and algebraic equations respectively. The vector dimensions are $\boldsymbol{x} \in \mathbb{R}^{4G}$, $\tilde{\boldsymbol{a}} \in \mathbb{R}^{2G}$, $\tilde{\boldsymbol{v}} \in \mathbb{R}^{2N}$, $\boldsymbol{a} \in \mathbb{R}^{2G+2N}$, $\boldsymbol{u} \in \mathbb{R}^{2G}$ yielding the nonlinear function mappings $\mathbf{f} : \mathbb{R}^{4G} \times \mathbb{R}^{2G+2N} \times \mathbb{R}^{2G} \to \mathbb{R}^{4G}$ and $\mathbf{g} : \mathbb{R}^{4G} \times \mathbb{R}^{2G+2N} \to \mathbb{R}^{(2G+2N)}$. The discretization methods to solve the NDAEs in (4) are discussed below.

B. Discretization for NDAE model

Implicit methods formulate sets of equations involving both current and future states of the system. When using implicit methods to solve NDAEs, each step of the numerical integration method is defined as a solution of a set of nonlinear equations. In this section, commonly used implicit methods such as Gear's and trapezoidal methods are discussed to solve the power systems NDAE model in (4). The time is discretized with step length h. Specifically, t takes the values t = nh where $n = 1, 2, \ldots n_p$, and $n_p = t_{\rm final}/h$ is the total number of time steps for a simulation horizon of $t_{\rm final}$ seconds.

1) Gear's method: To apply Gear's method for solving NDAEs, the model in (4) is rewritten as follows at time n:

$$\frac{\boldsymbol{x}(nh) - \sum_{s=1}^{k} \alpha_s \boldsymbol{x}(nh - sh)}{\beta h} = \boldsymbol{f}(\boldsymbol{x}(nh), \boldsymbol{a}(nh), \boldsymbol{u}(nh))$$
(5a)

$$\mathbf{0} = \mathbf{g}(\mathbf{x}(nh), \mathbf{a}(nh)) \tag{5b}$$

where the derivative is approximated using a linear combination of state values $\boldsymbol{x}(nh)$ and $\{\boldsymbol{x}(nh-sh)\}_{s=1}^k$ computed at k previous time steps. The constants β and α_s depend on the selected order k and are defined as follows:

$$\beta = \left(\sum_{s=1}^{k} \frac{1}{s}\right)^{-1}, \ \alpha_s = (-1)^{(s+1)} \beta \sum_{j=s}^{k} \frac{1}{j} \binom{j}{s}. \tag{6}$$

The set of equations in (5) amounts to a nonlinear system where $\boldsymbol{x}(nh)$ and $\boldsymbol{a}(nh)$ are unknown and must be solved. Eq. (5a) is rearranged and the following function is defined:

$$\psi(\boldsymbol{x}(nh), \boldsymbol{a}(nh), \boldsymbol{u}(nh)) = \boldsymbol{x}(nh) - \sum_{s=1}^{\kappa} \alpha_s \boldsymbol{x}(nh - sh) - h\beta \boldsymbol{f}(\boldsymbol{x}(nh), \boldsymbol{a}(nh), \boldsymbol{u}(nh))$$
(7)

2) Trapezoidal method: At time n, the model in (4) is rewritten as follows for the trapezoidal method:

$$\begin{split} \frac{\boldsymbol{x}(nh) - \boldsymbol{x}(nh-h)}{0.5h} &= (\boldsymbol{f}(\boldsymbol{x}(nh), \boldsymbol{a}(nh), \boldsymbol{u}(nh)) + \\ & \boldsymbol{f}(\boldsymbol{x}(nh-h), \boldsymbol{a}(nh-h), \boldsymbol{u}(nh-h))) \end{split} \tag{8a}$$

$$\mathbf{0} = \boldsymbol{g}(\boldsymbol{x}(nh), \boldsymbol{a}(nh)) \tag{8b}$$

Eq. (8a) is rearranged and the following function is defined:

$$\psi(\boldsymbol{x}(nh), \boldsymbol{a}(nh), \boldsymbol{u}(nh)) = \boldsymbol{x}(nh) - \boldsymbol{x}(nh-h) - 0.5h$$
$$[\boldsymbol{f}(\boldsymbol{x}(nh), \boldsymbol{a}(nh), \boldsymbol{u}(nh))$$
$$+ \boldsymbol{f}(\boldsymbol{x}(nh-h), \boldsymbol{a}(nh-h), \boldsymbol{u}(nh-h))]$$
(9)

The resulting system of equations for each method [cf. (5) or (8)] can be summarized as follows:

$$\mathbf{0} = \psi(\mathbf{x}(nh), \mathbf{a}(nh), \mathbf{u}(nh)) \tag{10a}$$

$$\mathbf{0} = \mathbf{g}(\mathbf{x}(nh), \mathbf{a}(nh)) \tag{10b}$$

where it is understood that $\psi(x(nh), a(nh), u(nh))$ also depends on state values prior to nh, depending on the definition and order of the discretization method. The PMU measurement model is discussed next.

C. PMU Measurement Model

Suppose that the N buses are connected to N_l lines. Let \mathcal{N}_j be the set of buses that are connected to the bus j, and $L_j = |\mathcal{N}_j|$ is defined as the number of lines that are connected to bus j. A PMU installed on bus j measures the bus complex voltage and complex line currents corresponding to all buses that are connected to bus j. PMUs are measuring quantities in rectangular coordinates. To formulate the expression for line currents, matrix \mathbf{Y}_{ft} is defined as

$$\mathbf{Y}_{ft} = \begin{bmatrix} \mathbf{Y}_f \\ \mathbf{Y}_t \end{bmatrix} \in \mathbb{R}^{2N_l \times N} \tag{11}$$

where Y_f and $Y_t \in \mathbb{R}^{N_t \times N}$ are *from* and *to* branch admittance matrices that can be easily extracted from MATPOWER [24]. The real and imaginary line currents are obtained as follows

$$\begin{bmatrix} \boldsymbol{i}_{R}(t) \\ \boldsymbol{i}_{I}(t) \end{bmatrix} = \begin{bmatrix} \operatorname{Re}[\boldsymbol{Y}_{ft}] & -\operatorname{Im}[\boldsymbol{Y}_{ft}] \\ \operatorname{Im}[\boldsymbol{Y}_{ft}] & \operatorname{Re}[\boldsymbol{Y}_{ft}] \end{bmatrix} \tilde{\boldsymbol{v}}(t)$$
(12)

A PMU that is installed on a bus *j* measures the following quantities

$$\boldsymbol{y}_{j} = \begin{bmatrix} v_{Rj} & v_{Ij} & \{i_{Rjk}\}_{k \in \mathcal{N}_{j}}^{T} & \{i_{Ijk}\}_{k \in \mathcal{N}_{j}}^{T} \end{bmatrix}^{T}$$
 (13)

where i_{Rjk} and i_{Ijk} are the real and imaginary currents corresponding to lines connected to bus j. Hence, the measurement vector \mathbf{y}_j at bus j can be written as

$$\mathbf{y}_{i} = \hat{\mathbf{C}}_{i}\tilde{\mathbf{v}} \tag{14}$$

with $\hat{m{C}}_j \in \mathbb{R}^{(2+2L_j) imes (2N)}$ defined as

$$\hat{C}_{j} = \begin{bmatrix} e_{j}^{T} & \mathbf{0} \\ \underline{0} & e_{j}^{T} \\ S_{j}Re(Y_{ft}) & -S_{j}Im(Y_{ft}) \\ S_{j}Im(Y_{ft}) & S_{j}Re(Y_{ft}) \end{bmatrix}$$
(15)

where e_j is the vector of standard basis in \mathbb{R}^N with 1 at row j and zero otherwise and $S_j \in \mathbb{R}^{L_j \times 2N_l}$ has 0/1 entries selecting the rows of Y_{ft} corresponding to lines connected to bus j [25].

The overall PMU measurement model can be written as

$$\mathbf{y}(t) = \hat{\mathbf{C}}\tilde{\mathbf{v}}(t) \tag{16}$$

where \hat{C} stacks all \hat{C}_j matrices corresponding to the installed PMUs. The measurement model is alternatively written as

$$y(t) = C\tilde{x}(t) \tag{17}$$

where $\tilde{\boldsymbol{x}}(t) = [\boldsymbol{x}(t)^T \ \boldsymbol{a}(t)^T]^T$ and matrix $\boldsymbol{C} = [\boldsymbol{O} \ \hat{\boldsymbol{C}}]$ has zero columns corresponding to all rows of $\tilde{\boldsymbol{x}}(t)$ except $\tilde{\boldsymbol{v}}(t)$.

The noisy version of y(t) is defined as

$$y(t) = C\tilde{x}(t) + w(t) \tag{18}$$

where w(t) represents zero-mean Gaussian noise assumed independent across the measurements.

The next section discusses the formulation of the Gauss-Newton method to perform DSE on the discretized NDAE model.

III. GAUSS NEWTON METHOD FOR NONLINEAR DYNAMIC STATE ESTIMATION

Given the NDAE model, and the implicit methods to discretize the model, the objective of this section is to estimate the states of the system (both dynamic and algebraic states, including ones not measured by PMUs). To this end, a nonlinear least squares problem is formulated and solved using the Gauss-Newton method to minimize the least squares objective function. Specifically, the dynamic and algebraic state values $\tilde{x}(t) = \tilde{x}(nh)$ are estimated for $n = 0, \ldots, n_p$. The vector z of all system states to be estimated is defined as

$$\boldsymbol{z} = \begin{bmatrix} \boldsymbol{x}(0)^T & \boldsymbol{a}(0)^T & \dots & \boldsymbol{x}(n_p h)^T & \boldsymbol{a}(n_p h)^T \end{bmatrix}^T$$
 (19a)

The residual function corresponding to the measurement equation at time nh is

$$\boldsymbol{r}_{\boldsymbol{y}}(nh) = \boldsymbol{y}(nh) - \boldsymbol{C}\tilde{\boldsymbol{x}}(nh) \tag{20}$$

where y(nh) is the vector of PMU measurements at each time sample, i.e., $\mathbf{y}(nh) = \mathbf{y}(t)$.

The residual functions corresponding to the discretized NDAE model are written as [cf. (10)]

$$\boldsymbol{r}_{xx}(nh) = \boldsymbol{\psi}(\boldsymbol{x}(nh), \boldsymbol{a}(nh), \boldsymbol{u}(nh))$$
 (21a)

$$\mathbf{r}_{xa}(nh) = \mathbf{g}(\mathbf{x}(nh), \mathbf{a}(nh)) \tag{21b}$$

where it is understood again that $r_{xx}(nh)$ also depends on previous state values depending on the definition and order of the discretization method.

Specifically, the residual functions of the discretization equations for Gear's method (5a)-(5b) are

$$r_{xx}(nh) = x(nh) - \sum_{s=1}^{k} \alpha_s x(nh - sh)$$
$$-h\beta f(x(nh), a(nh), u(nh))$$
(22a)

$$\mathbf{r}_{xa}(nh) = \mathbf{g}(\mathbf{x}(nh), \mathbf{a}(nh)) \tag{22b}$$

and the residual functions for the trapezoidal method (8a)–(8b) are

$$r_{xx}(nh) = \boldsymbol{x}(nh) - \boldsymbol{x}(nh - sh)$$
$$-0.5h\boldsymbol{f}(\boldsymbol{x}(nh), \boldsymbol{a}(nh), \boldsymbol{u}(nh)) \tag{23a}$$

$$\boldsymbol{r}_{xa}(nh) = \boldsymbol{g}(\boldsymbol{x}(nh), \boldsymbol{a}(nh)) \tag{23b}$$

The vector of residuals r(z) corresponding to all measurement, differential, and algebraic equations is defined as follows:

$$r(z) = \begin{bmatrix} r_y(0) \\ \vdots \\ r_y(n_p h) \\ r_{xa}(0) \\ r_{xx}(h) \\ r_{xa}(h) \\ \vdots \\ r_{xx}(n_p h) \\ r_{xa}(n_n h) \end{bmatrix}$$
(24)

The objective is to minimize the ℓ_2 -norm of the residual vector:

$$minimize ||r(z)||_2^2$$
 (25)

resulting in a nonlinear least squares problem that can be solved using the Gauss-Newton method. The advantage of the Gauss-Newton method is that it includes approximate Hessian information to iteratively update z, without actually formulating second-order derivatives of the objective function in (25).

The Jacobian matrix corresponding to (24) is defined as

$$J(z) = \begin{bmatrix} -M \\ N \end{bmatrix}$$
 (26)

where M is the Jacobian matrix of the residual function corresponding to the measurement equation in (20). Specifically, M is defined as a block diagonal matrix that contains n_n blocks of C.

Matrix N is the Jacobian matrix of the residual functions in (22a)–(22b) for Gear's method and (23a)–(23b) for the trapezoidal method. For both methods, matrix N \in $\mathbb{R}^{(2G+2N)+(4G+2G+2N)(n_p-1)\times(4G+2G+2N)n_p}$ has the following structure:

$$N = \begin{bmatrix} \Theta & O & O & O & O & \dots & O \\ \Phi & A_g & O & O & O & \dots & O \\ O & \Phi & A_g & O & O & \dots & O \\ \vdots & \vdots & \vdots & \ddots & \vdots & \ddots & O \\ O & O & O & O & \dots & \Phi & A_g \end{bmatrix}$$
(27)

where the block $[\Phi \ A_g]$ appears n_p times. Matrix $\Theta \in \mathbb{R}^{(2G+2N)\times (4G+2G+2N)}$ is defined as

$$\mathbf{\Theta} = \begin{bmatrix} \mathbf{G}_{\boldsymbol{x}}(\boldsymbol{x}(0), \boldsymbol{a}(0)) & \mathbf{G}_{\boldsymbol{a}}(\boldsymbol{x}(0), \boldsymbol{a}(0)) \end{bmatrix}$$
(28)

where G_x is the Jacobian matrix of (4b) with respect to state variables x, and G_a is the Jacobian matrix of (4b) with respect to algebraic variables a.

Matrix $\Phi \in \mathbb{R}^{(4G+2G+2N)\times(4G+2G+2N)}$ is defined for firstorder (k = 1) Gear's and trapezoidal methods as

$$\Phi = \begin{bmatrix} -I & O \\ O & O \end{bmatrix} \tag{29}$$

Matrix $oldsymbol{A_g} \in \mathbb{R}^{(4G+2G+2N) imes (4G+2G+2N)}$ is defined for Gear's method as

$$\mathbf{A}_{g} = \begin{bmatrix} \mathbf{I}_{x} - \beta h \mathbf{F}_{x} & -\beta h \mathbf{F}_{a} \\ \mathbf{G}_{x} & \mathbf{G}_{a} \end{bmatrix}$$
(30)

and for the trapezoidal method as

$$\boldsymbol{A_g} = \begin{bmatrix} \boldsymbol{I_x} - 0.5h\boldsymbol{F_x} & -0.5h\boldsymbol{F_a} \\ \boldsymbol{G_x} & \boldsymbol{G_a} \end{bmatrix}$$
(31)

where F_x is the Jacobian of (4a) with respect to state variables x, and F_a is the Jacobian matrix of (4a) with respect to algebraic variables $a;\ I_x$ is the identity matrix with same dimension as F_x . Matrices F_x , F_a , G_x , and G_a are evaluated at $\boldsymbol{x}(nh), \boldsymbol{a}(nh)$ for $n=1,\ldots,n_p$ corresponding to block rows of (27).

The Gauss-Newton update for iteration index γ is given as

$$\boldsymbol{z}^{(\gamma+1)} = \boldsymbol{z}^{(\gamma)} - h_{\boldsymbol{g}} (\boldsymbol{J}(\boldsymbol{z}^{(\gamma)})^{T} \boldsymbol{J}(\boldsymbol{z}^{(\gamma)}))^{-1} \boldsymbol{J}(\boldsymbol{z}^{(\gamma)})^{T} \boldsymbol{r}(\boldsymbol{z}^{(\gamma)})$$
(32)

where h_q is the stepsize of the method. The next section presents the relevant numerical results.

IV. NUMERICAL RESULTS

In this section, simulation results testing the performance of Gear's and trapezoidal methods in solving the DSE problem using the Gauss-Newton method are discussed. The simulations are performed in MATLAB R2021a on a 64-bit Windows 10 system equipped with a 3.5GHz Xeon^R E5-1650 CPU, and 128 GB of RAM. The MATLAB's ode15i solver (that solves the NDAE models) is used as a benchmark for DSE. The simulations are performed on the following test systems:

- Western System Coordinating Council (WECC) 3 machine, 9-bus system (referred to as *Case-9*)
- IEEE-57 test system consisting of 7 machines and 57 buses (referred as Case-57).

The machine constants and network parameters for all the cases are extracted from PST toolbox and MATPOWER respectively [23], [24]. Since the regulation and chest time constants are not specified in PST, their values are chosen to be $R_i = 0.02 \, \frac{({\rm Hz} \times rad)}{pu}$ and $T_{Chi} = 0.2 \, {\rm sec}$ [15]. The base power for all systems is 100 MVA and the synchronous speed of the network is $\omega_s = 2\pi 60 \, {\rm rad/sec}$. The generator parameters are obtained from case files data3m9b.m for Case-9. For Case-57 the machine constants are chosen based on the ranges of values provided in the PST toolbox. Parameter values for Case-57 have been selected as $M_i = 0.2 \, {\rm pu} \times {\rm sec}^2$, $D_i = 1.0 \, {\rm pu} \times {\rm sec}$, $x_{di} = 0.07 \, {\rm pu}$, $x_{qi} = 0.5 \, {\rm pu}$, $x_{di}' = 0.007 \, {\rm pu}$, and $T'_{doi}' = 5 \, {\rm sec}$.

Initial constant power loads (P_l^0, Q_l^0) are generated from MATPOWER based on the standard files given for the two networks. The algebraic variables a(0) at the initial operating point are calculated by solving the power flow equations using MATPOWER. The algebraic variables are then utilized to solve (1) upon setting $\dot{x} = 0$ together with (2) to obtain initial operating points of generators' dynamic states x(0) and control inputs u(0).

After t>0, an abrupt step disturbance is applied to the loads. The new values of complex power loads are specified as $P_l^d+jQ_l^d=(1+d)(P_l^0+jQ_l^0)$ where d is the magnitude of the disturbance. The initialization given to MATLAB's ode15i are the states and algebraic variables corresponding to the previous operating point computed before step disturbance is applied. The control inputs are obtained from MATPOWER's runopf.m based on the new loads.

Therefore, the simulated case amounts to a new command at generators based on the loads $P_l^d + jQ_l^d = (1+d)(P_l^0 + jQ_l^0)$ and the objective is to estimate the resulting dynamic and algebraic states from PMU measurements. A disturbance of 1% is considered for all the test cases. The order k=1 is chosen for Gear's method. The Gauss-Newton stepsize is selected as $h_q=0.1$.

The PMUs are installed on bus 4, 6, and 7 for *Case-9* [13], and for *Case-57* PMUs are installed on bus 1, 2, 4, 6, 9, 12, 15, 19, 20, 24, 25, 28, 29, 30, 32, and 33, 33, 35, 37, 38, 41, 46, 47, 50, 51, 53, 54, 56 [26]. Gaussian noise with standard deviation of 0.01, 0.02, and 0.05 i.e., 1%, 2%, and 5% noise is added to the measurements. All results are shown for step length h=0.1 and $t_{\rm final}=10$ sec.

The DSE results for Case-9 with 5% Gaussian noise under Gear's and trapezoidal (TRAP) methods are depicted in Fig. 1. The DSE results for Case-57 with 5% Gaussian noise under Gear's and trapezoidal methods are shown in Fig. 2. The generator states and the voltages in the figures converge to their steady state values and are estimated efficiently using the proposed method even under the effect of noise.

To assess the accuracy of the numerical methods, the root mean square error (RMSE) is calculated as

RMSE =
$$\sum_{m=1}^{4G+2G+2N} \sqrt{\frac{1}{n_p} \sum_{n=0}^{n_p} (e_m[n])^2}$$
 (33)

where $e_m[n]$ is the error between MATLAB's ode15i solver

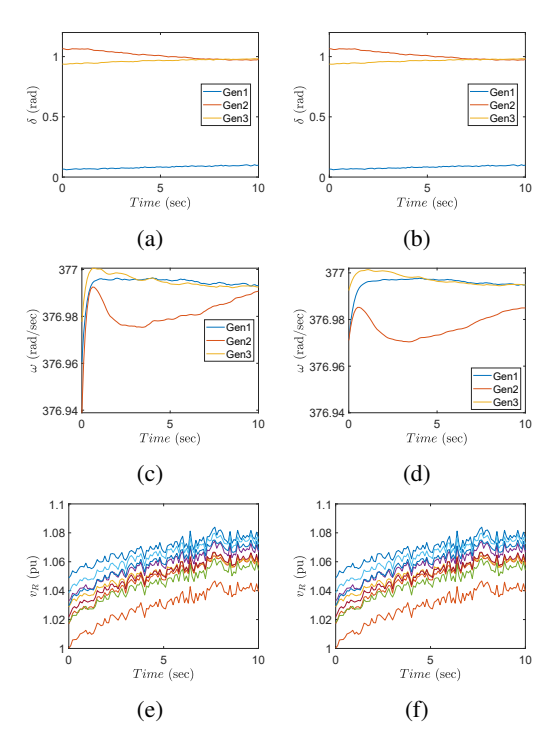


Fig. 1: Estimated generator angles, frequencies, and bus voltages with 5% noise for *Case-9* using Gear's method (left) and trapezoidal method (right).

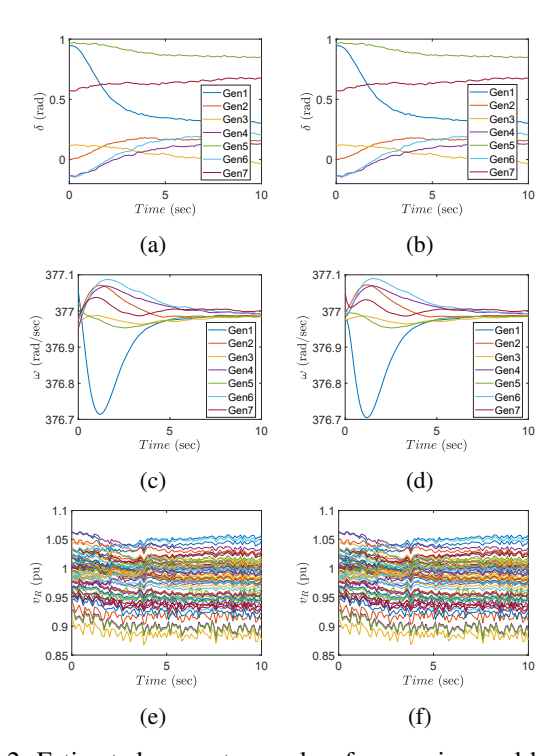


Fig. 2: Estimated generator angles, frequencies, and bus voltages with 5% noise for *Case-57* using Gear's method (left) and trapezoidal method (right).

TABLE I: RMSE values of numerical methods solving DSE using Gauss-Newton method at step length h=0.1 and time span 10 seconds.

Test Case	Numerical Method	Without noise	
	Gear (k=1)	0.0144	
Case-9	TRAP	0.0015	
	Gear (k=1)	0.4782	
Case-57	TRAP	0.0150	

TABLE II: RMSE values averaged over 10 noise realizations at step length h=0.1 and time span 10 seconds.

Test Case	Numerical Method	with 1% noise	with 2% noise	with 5% noise
	Gear (k=1)	0.5134	1.5571	2.0758
Case-9	TRAP	0.3010	1.0389	1.4841
	Gear (k=1)	1.2830	2.2561	4.9912
Case-57	TRAP	1.0595	2.0419	4.7596

and the DSE method using Gear's and trapezoidal discretizations and m indexes all network states and algebraic variables at time n. The RMSE values for the DSE without noise are listed in Table I. The RMSE values averaged over 10 noise realization sequences are listed in Table II for different noise standard deviations. It is worth noting that the trapezoidal method is characterized by lower RMSE values compared to Gear's method for both test systems.

V. CONCLUSION

In this paper, a method to perform DSE based on discretized NDAE models of power systems has been developed. The DSE objective amounts to a nonlinear least squares problem that can be solved using the Gauss-Newton method. The simulation results for DSE with discretized NDAEs show that the method is accurate, robust under the effect of noise, and works efficiently. The trapezoidal method has better performance compared to Gear's method. Future work includes accommodating renewable generation dynamics into the NDAE model and analyzing how to implement the developed DSE model in a rolling window fashion.

REFERENCES

- F. Milano, Power system modelling and scripting. Springer Science & Business Media, 2010.
- [2] B. Stott, "Power system dynamic response calculations," Proceedings of the IEEE, vol. 67, no. 2, pp. 219–241, 1979.
- [3] E. Süli, "Numerical solution of ordinary differential equations," Mathematical Institute, University of Oxford, 2010.
- [4] F. Milano, "Semi-implicit formulation of differential-algebraic equations for transient stability analysis," *IEEE Transactions on Power Systems*, vol. 31, no. 6, pp. 4534–4543, 2016.
- [5] D. Yang and V. Ajjarapu, "A decoupled time-domain simulation method via invariant subspace partition for power system analysis," *IEEE Transactions on Power Systems*, vol. 21, no. 1, pp. 11–18, 2006.
- [6] R. Yao, Y. Liu, K. Sun, F. Qiu, and J. Wang, "Efficient and robust dynamic simulation of power systems with holomorphic embedding," *IEEE Transactions on Power Systems*, vol. 35, no. 2, pp. 938–949, 2019.
- [9] S. Nugroho, A. F. Taha, T. Summers, and N. Gatsis, "Simultaneous sensor and actuator selection/placement through output feedback control," in 2018 annual American control conference (ACC). IEEE, 2018, pp. 4159–4164.

- [7] C.-W. Liu and J. S. Thorp, "New methods for computing power system dynamic response for real-time transient stability prediction," *IEEE Transactions on Circuits and Systems I: Fundamental Theory and Applications*, vol. 47, no. 3, pp. 324–337, 2000.
- [8] C. W. Gear, "Towards explicit methods for differential algebraic equations," BIT Numerical Mathematics, vol. 46, no. 3, pp. 505–514, 2006.
- [10] J. Qi, A. F. Taha, and J. Wang, "Comparing kalman filters and observers for power system dynamic state estimation with model uncertainty and malicious cyber attacks," *IEEE Access*, vol. 6, pp. 77 155–77 168, 2018.
- [11] J. Zhao, M. Netto, and L. Mili, "A robust iterated extended kalman filter for power system dynamic state estimation," *IEEE Transactions* on *Power Systems*, vol. 32, no. 4, pp. 3205–3216, 2016.
- [12] S. Jin, Z. Huang, R. Diao, D. Wu, and Y. Chen, "Comparative implementation of high performance computing for power system dynamic simulations," *IEEE Transactions on Smart Grid*, vol. 8, no. 3, pp. 1387–1395, 2017.
- [13] S. A. Nugroho, A. Taha, N. Gatsis, and J. Zhao, "Observers for differential algebraic equation models of power networks: Jointly estimating dynamic and algebraic states," *IEEE transactions on control of network* systems, 2022.
- [14] A. Minot, Y. M. Lu, and N. Li, "A distributed gauss-newton method for power system state estimation," *IEEE Transactions on Power Systems*, vol. 31, no. 5, pp. 3804–3815, 2015.
- [15] M. Bazrafshan, N. Gatsis, A. F. Taha, and J. A. Taylor, "Coupling load-following control with opf," *IEEE Transactions on Smart Grid*, vol. 10, no. 3, pp. 2495–2506, 2018.
- [16] M. E. Baran and A. W. Kelley, "State estimation for real-time monitoring of distribution systems," *IEEE Transactions on Power Systems*, vol. 9, no. 3, pp. 1601–1609, 1994.
- [17] H. Cevallos, G. Intriago, and D. Plaza, "Performance of the estimators weighted least square, extended kalman filter, and the particle filter in the dynamic estimation of state variables of electrical power systems," in 2018 IEEE International Conference on Automation/XXIII Congress of the Chilean Association of Automatic Control (ICA-ACCA), 2018, pp. 1–6
- [18] H. M. Beides and G. T. Heydt, "Dynamic state estimation of power system harmonics using kalman filter methodology," *IEEE Transactions* on *Power Delivery*, vol. 6, no. 4, pp. 1663–1670, 1991.
- [19] A. Rouhani and A. Abur, "Linear phasor estimator assisted dynamic state estimation," *IEEE Transactions on Smart Grid*, vol. 9, no. 1, pp. 211–219, 2016.
- [20] H. H. Alhelou, M. E. H. Golshan, and N. D. Hatziargyriou, "Deterministic dynamic state estimation-based optimal lfc for interconnected power systems using unknown input observer," *IEEE Transactions on Smart Grid*, vol. 11, no. 2, pp. 1582–1592, 2019.
- [21] X. Li, A. Scaglione, and T.-H. Chang, "A framework for phasor measurement placement in hybrid state estimation via gauss–newton," *IEEE Transactions on Power Systems*, vol. 29, no. 2, pp. 824–832, 2013.
- [22] S. Sarri, L. Zanni, M. Popovic, J.-Y. Le Boudec, and M. Paolone, "Performance assessment of linear state estimators using synchrophasor measurements," *IEEE Transactions on Instrumentation and Measure*ment, vol. 65, no. 3, pp. 535–548, 2016.
- [23] P. W. Sauer, M. A. Pai, and J. H. Chow, *Power system dynamics and stability: with synchrophasor measurement and power system toolbox*. John Wiley & Sons, 2017.
- [24] R. D. Zimmerman, C. E. Murillo-Sánchez, and R. J. Thomas, "Mat-power: Steady-state operations, planning, and analysis tools for power systems research and education," *IEEE Transactions on power systems*, vol. 26, no. 1, pp. 12–19, 2010.
- [25] V. Kekatos, G. B. Giannakis, and B. Wollenberg, "Optimal placement of phasor measurement units via convex relaxation," *IEEE Transactions* on power systems, vol. 27, no. 3, pp. 1521–1530, 2012.
- [26] S. Chakrabarti and E. Kyriakides, "Optimal placement of phasor measurement units for power system observability," *IEEE Transactions on power systems*, vol. 23, no. 3, pp. 1433–1440, 2008.